

脱水 Ni-Fe 类水滑石的制备及其作为环保型催化剂 用于生物质糠醛的高选择性缩醛化反应

程淑艳^{1,2,3} 寇佳伟^{*1} 程芳琴³

(¹太原理工大学省部共建煤基能源清洁高效利用国家重点实验室,太原 030024)

(²山西大学环境与资源学院,太原 030013)

(³山西大学山西省黄河实验室,太原 030013)

摘要: 合成了含硝酸根离子的脱水 Ni-Fe 类水滑石(Ni-Fe HTLCs)并将其应用于室温下的糠醛缩醛化反应。脱水 Ni-Fe HTLCs 对糠醛缩醛化反应显示出高选择性并基本实现糠醛的完全转化。作为耐水的路易斯酸和脱水剂,脱水 Ni-Fe HTLCs 被证明是适用于糠醛缩醛化反应的高效双功能催化剂。通过研究发现,脱除 Ni-Fe HTLCs 中水分导致颗粒收缩并增强层板间硝酸根离子间的电荷互斥, Ni-Fe HTLCs 中弱酸性位点在糠醛缩醛化中发挥重要作用,脱水可改变酸性位点结构并增强其活性。脱水 Ni-Fe HTLCs 可吸收缩醛化反应中产生的大部分水分,但吸水后 Ni-Fe HTLCs 的结构并不能完全恢复,这可能是由扩散进入 HTLCs 层板间的有机分子导致。

关键词: 类水滑石; 糠醛; 缩醛; 双功能催化剂; 生物油

中图分类号: O614.81¹; O614.81³; TQ215 文献标识码: A 文章编号: 1001-4861(2021)11-2092-09

DOI:10.11862/CJIC.2021.220

Preparation of Dehydrated Ni-Fe Hydrotalcite-like Compounds as an Eco-Friendly Catalyst for Highly Selective Acetalization of Biomass-Derived Furfural

CHENG Shu-Yan^{1,2,3} KOU Jia-Wei^{*1} CHENG Fang-Qin³

(¹State Key Laboratory of Clean and Efficient Coal Utilization, Taiyuan University of Technology, Taiyuan 030024, China)

(²College of Environmental & Resource Science, Shanxi University, Taiyuan 030013, China)

(³Shanxi Laboratory for Yellow River, Shanxi University, Taiyuan 030013, China)

Abstract: The dehydrated Ni-Fe hydrotalcite-like compounds (Ni-Fe HTLCs) containing nitrate anions were synthesized and applied in furfural acetalization at room temperature. The dehydrated Ni-Fe HTLCs showed good selectivity for furfural acetalization and achieved almost complete conversion of furfural. The dehydrated Ni-Fe HTLCs as water-tolerant Lewis acids and water scavengers was proved to be an efficient bifunctional catalyst for furfural acetalization. The removal of interlayer water leads to shrinkage of Ni-Fe HTLCs particles and increase in electronic repulsion among NO₃⁻ ions in the interlayer. The weak acid sites in Ni-Fe HTLCs play an important role in furfural acetalization. The dehydration changes structure of the acid sites and thus improves activity of the weak acid sites. The dehydrated Ni-Fe HTLCs can absorb the most of the resulting water during furfural acetalization, but the structure of Ni-Fe HTLCs cannot completely recover after rehydration possibly due to hindering effect of organic molecules diffusing into interlayer space.

Keywords: hydrotalcite-like compound; furfural; acetal; bifunctional catalyst; bio-oil

收稿日期:2021-04-18。收修改稿日期:2021-08-09。

国家自然科学基金(No.22108161)和山西省青年科学基金(No.201901D211297)资助。

*通信联系人。E-mail:koujiawei@tyut.edu.cn

0 Introduction

The conversion of biomass, such as agricultural and forest residues, into biofuel and value-added chemicals is one of the most sustainable routes to decrease the dependency on fossil fuels and thus to control CO₂ emissions^[1]. The bio-oil contains more than 400 organics compounds such as guaiacols, phenols, furfural and their derivatives^[2]. The furfural (about 4%) in lignocellulosic bio-oil can undergo polymerization at high concentrations, and the furfural can polymerize with phenols to form phenol-furfural resin at high temperatures^[3]. Therefore, it is necessary to convert furfural into stable substances under mild conditions for stabilization and industrial application of bio-oil.

Acetalization reactions are viable routes to protect formyl groups in furfural. The furfural acetals (*e.g.*, furfural propyleneglycol acetal and furfural glycol acetal) can be extracted from bio-oil as flavouring food additives, plant growth regulator, and high-performance fuel additives^[4]. Conventionally, formation of furfural acetal involves straight forward reaction of furfural with 1,2- or 1,3-diol catalyzed by Brønsted or Lewis acids under reflux conditions. However, it is inevitable that the unwanted homopolymerization and copolymerization reactions of furfural in bio-oil are accelerated at elevated temperatures. Moreover, α , β - unsaturated aldehydes such as furfural are labile at elevated temperatures, and thus the furfural acetalization with 1,2-diol under reflux conditions will lead to a mixture of by-products and poor yield of the desired acetal^[5]. In recent years, it is reported that the direct acetalization of aldehyde with diol can undergo over solid acid catalysts at ambient temperature, and trichloroacetonitrile served as a water scavenger under mild acidic conditions^[6], but the highly toxic trichloroacetonitrile is possible to result in environmental pollution. An eco-friendly method should be developed for furfural acetalization under mild conditions.

In general, furfural acetalization is catalyzed by protonic acids (*i.e.*, HCl or H₂SO₄)^[7], which result in a series of problems such as large generation of effluents, complex purification of products, difficult neutralization of residues and serious corrosion of equipments^[8].

The use of the Brønsted acid catalysts raises serious environmental matters. Therefore, to deal with these environmental problems resulted from the homogeneous Brønsted acid catalysts, a lot of attention has been recently attracted to the development of environmentally-friendly heterogeneous catalysts. Several solid acids (*e.g.*, cerium chloride^[9], cerium phosphate^[10] and propyl phosphonic anhydride^[11]) have been used as catalysts in the furfural acetalization. Although benign to the environment, these catalysts sometimes suffer leaching problems or deactivation^[7]. Accordingly, these solid acids catalysts are not easy to be reused. The use of transition-metal Lewis acids containing Pd^[12] or Rh^[13] obtain good results for the acetalization reactions, but the noble metal catalysts are very expensive and usually unstable^[14]. Thus, the Lewis acid catalysts with noble metals are difficult to be applied in an industrial scale. In brief, the development of an eco-friendly catalyst that is easily separable, reusable, and stable has been long-expected for the acetalization reactions.

Hydrotalcite-like compounds (HTLCs), a kind of layered double hydroxides (LDHs), have a network of double-layer structure with mesopores and/or micropores, and anions between the layers and cations in their layers are exchangeable. Generally, their composition is represented by the following formula^[15]: $[M_{1-x}^{2+}M_x^{3+}(\text{OH})_2]^{x+}[A_{x/n}^{n-}] \cdot m\text{H}_2\text{O}$, where divalent cation (M^{2+}) may be Mn²⁺, Cu²⁺ or Zn²⁺, *etc.*; trivalent cation (M^{3+}) may be Al³⁺, Ga³⁺ or Cr³⁺, *etc.*; anion (A^{n-}) may be CO₃²⁻, NO₃⁻, OH⁻, *etc.*; x ($0.2 \leq x \leq 0.33$) is the trivalent cation substitution degree in the hydroxy layer^[16]. Besides anions intercalating between the brucite-type layers, crystallization water molecules ($m\text{H}_2\text{O}$) into interlayers connect the hydroxyl groups of the brucite-type layers through hydrogen bonds^[17]. HTLCs are widely used as photoelectric material, catalysts, and precursor of composite materials^[18]. An unusual feature of HTLCs is the memory effect. The water molecules in interlayer of HTLCs can be removed by heating, and the dehydrated HTLCs can recover the original hydrotalcite structure by absorbing water^[19]. Accordingly, we anticipated that the dehydrated HTLCs can play a dual role as a Lewis acid catalyst and a water scavenger dur-

ing furfural acetalization.

In our present work, Ni-Fe HTLCs were prepared by a co-precipitation method. Subsequently, the dehydrated Ni-Fe HTLCs were systematically characterized, and their catalytic performance for furfural acetalization was evaluated. The objective of this work was to investigate the effects of structure and properties on catalytic performance of the dehydrated Ni-Fe HTLCs for the furfural acetalization.

1 Experimental

1.1 Preparation

According to Ni/Fe molar ratios of 2.0, 60 mL of $\text{Ni}(\text{NO}_3)_2$ and 30 mL of $\text{Fe}(\text{NO}_3)_3$ aqueous solutions ($1.0 \text{ mol}\cdot\text{L}^{-1}$) were mixed in a beaker. Subsequently, NaOH ($1.0 \text{ mol}\cdot\text{L}^{-1}$) and Na_2CO_3 ($0.5 \text{ mol}\cdot\text{L}^{-1}$) aqueous solutions with appropriate volume were simultaneously and dropwise added into the mixture containing $\text{Ni}(\text{NO}_3)_2$ and $\text{Fe}(\text{NO}_3)_3$ under continuously stirring. The precipitation reaction was carried out at a constant pH value ($\text{pH}=5.4\pm 0.3$). The obtained slurry was aged at $110\text{ }^\circ\text{C}$ for 4 h in a hydrothermal autoclave, and then the precipitate was separated by filtration and rinsing with deionized water. Afterwards, the leached powder was dried at $80\text{ }^\circ\text{C}$ for 2 h under vacuum to obtain the as-synthesized Ni-Fe HTLCs (HT-as) without physically adsorbed water. HT-as was dried at $150\text{ }^\circ\text{C}$ for 2 h under vacuum to remove interlayer water and thus to obtain the dehydrated Ni-Fe HTLCs (HT-dh).

1.2 Characterization

Powder X-ray diffraction (XRD) patterns of the samples were recorded in the 2θ range of 5° - 80° at a speed of $8\text{ }^\circ\cdot\text{min}^{-1}$ on a D/max-2500 X-ray diffractometer (Rigaku Co., Ltd., Japan) with $\text{Cu K}\alpha$ radiation ($\lambda=0.154 \text{ nm}$). The operating voltage and current were 30 kV and 100 mA, respectively.

The diffuse reflectance infrared Fourier transformation (DRIFT) spectra were recorded on a Vertex-70 infrared spectrometer (Bruker Co., Ltd., Germany) over a co-addition of 200 scans at 4 cm^{-1} resolution, and the sample was placed in a 0030-102 diffuse reflectance cell (Pike Co., Ltd., USA) equipped with ZnSe windows. Before the infrared measurement was performed,

the diffuse reflectance cell was vacuumized to eliminate the moisture in the atmosphere and water adsorbed on the surface of the samples, and then high purity argon (99.999%) was introduced as protection gas.

Ammonia temperature programmed desorption (NH_3 -TPD) was measured on a ChemBET-3000 absorption apparatus (Quantachrome Co., Ltd., USA). The samples (0.05 g) were loaded in a quartz vessel and then thermostated at $100\text{ }^\circ\text{C}$ for 0.5 h. The vessel was cooled down to $50\text{ }^\circ\text{C}$. After the surface of the sample was completely adsorbed and saturated in ammonia at $50\text{ }^\circ\text{C}$, the temperature of the sample was increased from 50 to $500\text{ }^\circ\text{C}$ at a rate of $10\text{ }^\circ\text{C}\cdot\text{min}^{-1}$ by a temperature-programmed controller. The tail gas was analyzed by a thermal conductivity detector (TCD). To eliminate the disturbance of produced H_2O and NO_x during decomposition of Ni-Fe HTLCs, TCD signals of the same samples (0.05 g) without ammonia were recorded under the same testing condition prior to NH_3 -TPD measurement, and the signals of the blank test as background signals were subtracted from original NH_3 -TPD profiles.

The specific surface area (S_{BET}), pore volume (V_{BHH}) and average pore diameter (D_{ave}) were measured by static nitrogen adsorption-desorption on a QDS-30 physisorption instrument (Quantachrome Co., Ltd., USA) at $-196\text{ }^\circ\text{C}$. Prior to test, the samples were degassed at $200\text{ }^\circ\text{C}$ for 4 h.

The thermogravimetric (TG) and the differential thermogravimetric (DTG) curves were measured in argon gas on a Setsys Evolution thermogravimetry (Setaram Co., Ltd., French) at a heating rate of $10\text{ }^\circ\text{C}\cdot\text{min}^{-1}$ from room temperature to $1\ 000\text{ }^\circ\text{C}$.

Scanning electron microscopy (SEM) characterization was performed at 20 kV on a JSM-6010plus/LV scanning electron microscope (Japan Electron Optics Laboratory Co., Ltd., Japan) to observe the morphology and microstructure of the samples pretreated by sputtered Au.

1.3 Evaluation

Furfural reacted with ethylene glycol to form furfural glycol acetal (FGA) under mild reaction conditions. In this work, the solvents and reactants were analytical

grade (mass ratio of *ca.* 99%). Furfural and ethylene glycol were purchased from Sigma - Aldrich. Prior to being used, furfural was freshly distilled with collection of the middle fraction under reduced pressure and then stored under a nitrogen atmosphere. To prevent hydrolysis of the formed acetal, the syntheses were performed in an excess of ethylene glycol aiming to shift the equilibrium toward the desired acetal. In addition, the excessive ethylene glycol can combine with water by hydrogen bonding and thus prevented hydrolysis of the acetal. The excessive ethylene glycol served as solvent and dehydrant. Despite the large excess, the ethylene glycol can be recovered by vacuum distillation and reused in another reaction. In a general procedure, a mixture of furfural (9.61 g), ethylene glycol (62.1 g) and HT-dh (36.0 g) was added in a three-neck flask equipped with a thermostat and a magnetic stirrer, and then the mixture was vigorously stirred for 7 h at 25 °C. HT-dh served as a catalyst and a water scavenger during furfural acetalization. Highly pure nitrogen gas (99.999%) was used as protection gas. As a contrast, the mixture containing 5 mL of cyclohexane as an entrainer was refluxed at 100 °C for 7 h, and the resulting water was separated by a Dean-Stark trap. The sampling was conducted at intervals of 1 h. Ni-Fe HTLCs were recycled from the reaction mixture by filtration and by washing with dichloromethane, and then the samples were dried at 80 °C under vacuum to obtain the rehydrated Ni-Fe HTLCs (HT-rh) during the furfural acetalization reaction. The residual organic mixture was dried with anhydrous magnesium sulfate, filtered and concentrated under reduced pressure. The components of the mixture were analyzed on an Agilent 7890B gas chromatograph (Agilent Technologies Co. Ltd., USA) equipped with a flame ionization detector (FID) and an OV - 101 capillary column (0.2 mm×50 m). The column was heated from 50 to 160 °C at a rate of 5 °C · min⁻¹. The temperatures of injector and FID were 200 and 230 °C, respectively. The sampling volume was 0.2 μL. The furfural conversion (*X*) and FGA selectivity (*S*) were calculated according to the following equations:

$$X = \frac{n_f - n_p}{n_f} \times 100\% \quad (1)$$

$$S = \frac{n_b}{n_i} \times 100\% \quad (2)$$

where n_f (mol) and n_p (mol) are the amounts of furfural in reactants and products, respectively; n_b (mol) is amount of FGA in products; n_i is total amounts of various organic products.

The water content of the freshly prepared mixture was measured on a Tracera GC - 2010 Plus (Shimadzu Scientific Instruments, Japan) equipped with a Watercol 1910 capillary column (0.32 mm×30 m) and a thermal conductivity detector (TCD). The samples and TCD were heated up to 150 and 250 °C, respectively, and the carrier gas was helium at 1.5 mL · min⁻¹ with a split ratio of 100:1.

2 Results and discussion

2.1 Structural and morphological analyses of Ni-Fe HTLCs catalysts

As shown in Fig.1, HT-as (Fig.1a) exhibits diffraction peaks at approximately $2\theta=9.9^\circ$, 20.2° , 34.5° , and 61.4° , which can be assigned (003), (006), (009) and (110) reflections of HTLCs, respectively^[20]. No other diffraction peak was detected in the XRD patterns, indicating high purity of the crystalline phases. Removal of interlayer water in HT-dh was evidenced by the shift of (003) diffraction peak from $2\theta=9.9^\circ$ to $2\theta=11.9^\circ$ (Fig.1b). In addition, the (003) diffraction peak of HT-dh broadened in comparison with HT-as, suggesting long-range ordering in Ni-Fe HTLCs is decreased after dehydration. The intensity of the characteristic (006), (009), and (113) reflections of HT - dh at $2\theta=21.7^\circ$, 35.8° , and 62.6° , respectively, decreased remarkably in comparison with HT - as, which implies an important disorder in the stacking of the layers in the dehydrated sample. The (003) diffraction peak began to sharpen again after rehydration (Fig. 1c), which reveals that rehydration involves not only the physical diffusion of water molecules into the interlayer space of Ni-Fe HTLCs, but also a phase transition from the disordered dehydrated phase back to the original ordered hydrotalcite. The XRD patterns of HT-as (Fig. 1a) and HT-rh (Fig. 1c) were very similar except that the intensity of the diffraction peaks for HT-rh was

slightly lower than the intensity for HT-as, indicating incomplete recovery of hydrotalcite structure after rehydration during the furfural acetalization reaction.

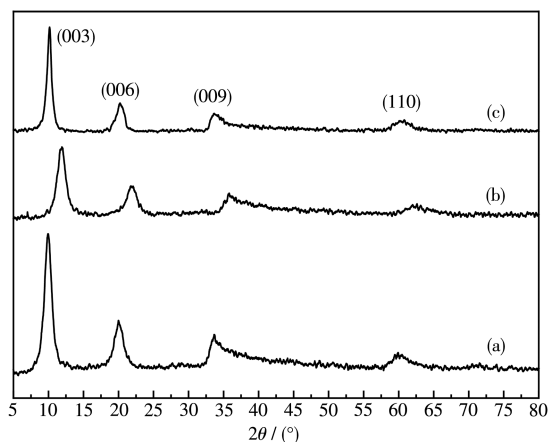


Fig.1 XRD patterns of HT-as (a), HT-dh (b), and HT-rh (c)

The XRD patterns showed that Ni-Fe HTLCs have a typical layered structure with 3R symmetry of HTLCs, which agrees well with the results reported in previous literature^[21]. Assuming a hexagonal 3R stacking sequence of adjacent brucite-type layers, the parameters a and c can be obtained from basal spacing of crystal planes (110) ($d_{(110)}$) and (003) ($d_{(003)}$), respectively ($c=3d_{(003)}$; $a=2d_{(110)}$). The parameter a is used as a quantitative measure of the intermetallic average distance^[16]. The parameter c relates to the distance between a brucite-type layer and an interlayer, which depends on the size of interlayer anions and/or electrostatic forces between cations in the layers and interlayer anions^[22]. As shown in Table 1, the parameter a was not altered significantly upon dehydration, the changes in the parameter c were observed in the following order: HT-dh < HT-rh < HT-as. The parameter c decreased from 2.583 nm for HT-as down to 1.626 nm for HT-dh after dehydration, which was equivalent to shrinkage of the interlayer space in HT-dh by 37% in comparison with HT-as. The parameters c increased to

Table 1 Crystallographic data calculated by XRD results

Sample	$d_{(003)}$ / nm	$d_{(110)}$ / nm	a / nm	c / nm	D / nm
HT-as	0.861	0.159	0.318	2.583	7.295
HT-dh	0.542	0.155	0.310	1.626	4.961
HT-rh	0.775	0.157	0.314	2.325	6.931

2.325 nm for HT-rh. Namely, about 90% of interlayer space was recovered after rehydration. The average crystallite size (D) of the samples was estimated by the Scherrer method. In comparison with HT-as, the crystallite size approximately decreased by 32% and 5% for HT-dh and HT-rh, respectively.

The DRIFT measurements were taken to understand the structure of Ni-Fe HTLCs, and the infrared spectra were shown in Fig.2. For HT-as and HT-rh samples (Fig.2a and 2c), the broad band was observed at $3\ 454\ \text{cm}^{-1}$, which is attributed to the stretching of hydrogen-bonded hydroxyl groups in the interlamellar water molecules and the brucite-type layers^[23]. The bands at $1\ 047$ and $825\ \text{cm}^{-1}$ are assigned to the deformation mode of Ni—OH and Al—OH^[24]. The bands centered at $1\ 386\ \text{cm}^{-1}$ correspond to the stretching of NO_3^- ions^[25]. For HT-dh (Fig.2b), the maximum of the broad band shifted from $3\ 454$ to $3\ 620\ \text{cm}^{-1}$, indicating the presence of isolated hydroxyl groups in the layer of the dehydrated Ni-Fe HTLCs. In addition, the band centered at $1\ 386\ \text{cm}^{-1}$ was split into two bands centered at $1\ 382$ and $1\ 324\ \text{cm}^{-1}$, indicating that the decrease in the interlayer space of Ni-Fe HTLCs leads to the reorganization of the NO_3^- anions in the interlayer. The band at $1\ 324\ \text{cm}^{-1}$ is due to the conversion of symmetry from D_{3h} in HT-as to C_s , C_{3v} , or C_{2v} symmetry in HT-dh^[26]. The lower symmetry degree of NO_3^- ions in HT-dh may result from the restricted freedom degree of the NO_3^- ions in the confined interlayer space and the increase in electronic repulsion among NO_3^- ions in the absence of water. No band of organic molecules was

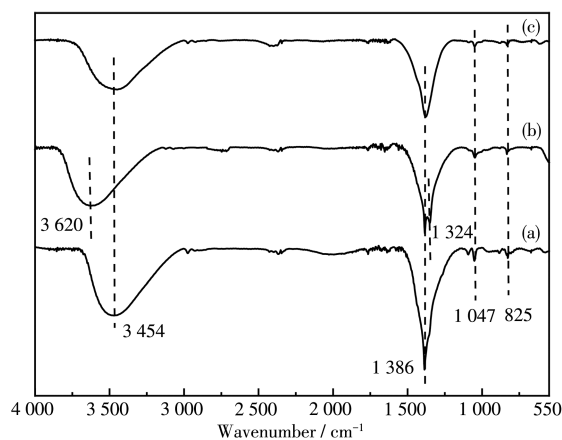


Fig.2 DRIFT spectra of HT-as (a), HT-dh (b), and HT-rh (c)

detected in the infrared spectra, indicating that the adsorbed organic compounds were removed completely.

The textural properties of samples are summarized in Table 2. The pore sizes of all the samples were in a range of 2-50 nm, and thus Ni-Fe HTLCs were regarded as mesoporous materials. HT-dh presented an obvious decrease in S_{BET} , V_{BJH} and D_{ave} compared to HT-as due to the particle shrinkage after dehydration. For HT-rh, a slight decrease in the S_{BET} , V_{BJH} and D_{ave} was detected in comparison with HT-as, indicating that the physical structure of Ni-Fe HTLCs cannot be completely recovered after rehydration during furfural acetalization reaction.

Table 2 Textural properties of the catalysts

Catalyst	$S_{\text{BET}} / (\text{m}^2 \cdot \text{g}^{-1})$	$V_{\text{BJH}} / (\text{cm}^3 \cdot \text{g}^{-1})$	$D_{\text{ave}} / \text{nm}$
HT-as	38	0.082	19.77
HT-dh	26	0.061	15.81
HT-rh	31	0.073	17.43

2.2 Thermal stability of Ni-Fe HTLCs

As shown in the TG-DTG curves of HT-as (Fig.3), there were three regions where the loss of weight occurred: (1) 5% of weight loss between 40 and 87 °C due to the removal of physisorbed water; (2) 13% in the range of 87-257 °C due to the removal of interlayer water; (3) 43% for the temperature interval of 257-556 °C due to thermal decomposition of NO_3^- ions and dehydroxylation. The first and second weight-loss steps are not separated clearly by a well-defined plateau. The removal rate of interlayer water reached to a maximum at 140 °C, and 13% mass of Ni-Fe HTLCs was lost after dehydration.

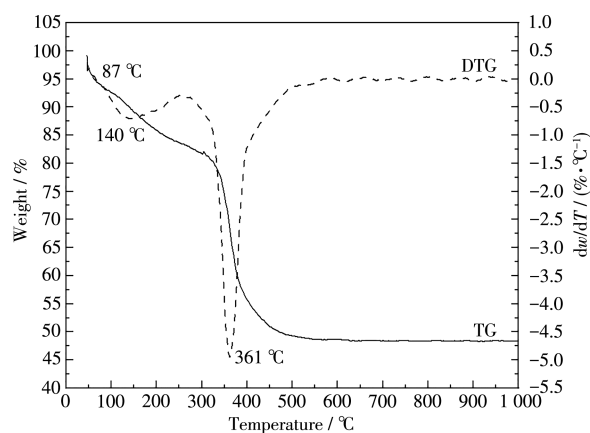
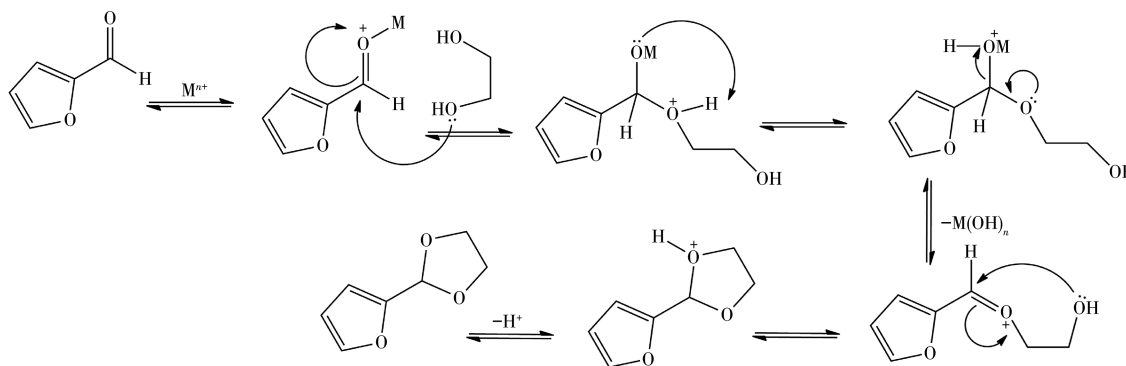


Fig.3 TG-DTG curves of HT-as

2.3 Surface acidity of Ni-Fe HTLCs

Generally, the acetalization reaction was catalyzed by Brønsted acids or Lewis acids. Based on experimental results and literature^[7], a plausible mechanistic proposal involving the metal cations in a layer of Ni-Fe HTLCs is depicted in Scheme 1. Therefore, the cations as Lewis acids on the surface of Ni-Fe HTLCs should be the catalytic active sites, and the surface acidity of Ni-Fe HTLCs catalysts was analyzed. As shown in Fig.4, the NH_3 -TPD profiles suggest a significant concentration of acidic sites on the surface of all the samples. The desorption peaks in the range of 50-250 °C were attributed to weak acidic sites of Ni-Fe HTLCs catalysts, and the peaks in the range of 250-380 °C were ascribed to strong acidic sites. The relative areas of the desorption peaks of HT-dh were significantly higher than those of HT-rh and HT-as, but the specific surface area of HT-dh was smaller than HT-rh and HT-as, indicating higher acidity of Lewis acidic



Scheme 1 Proposed reaction mechanism of furfural acetalization catalyzed by Ni-Fe HTLCs

(M^{n+} represents metal cations in layers of Ni-Fe HTLCs)

sites in absence of interlayer water. In comparison with HT-rh and HT-as, the peak shape of weak acidic sites for HT-dh began to sharpen, and the peak maximum of the weak acidic sites shifted from 124 to 155 °C after dehydration, suggesting that dehydration leads to the change in structure of weak acidic sites in layers of Ni-Fe HTLCs. H_2O and NO_3^- anions in the interlayer of Ni-Fe HTLCs are directly coordinated to the matrix Ni^{2+} cations in layers of Ni-Fe HTLCs through oxygen atoms. The removal of interlayer water may lead to a structural rearrangement of the metal complex. Accordingly, the interlayer water molecules increase electronic cloud density of the metal cations (*i.e.*, decrease in the acidity of Lewis acidic sites) by coordinating with metal cations, and thus their electronic cloud density decrease after dehydration, namely the increase in combining capacity with electron donors.

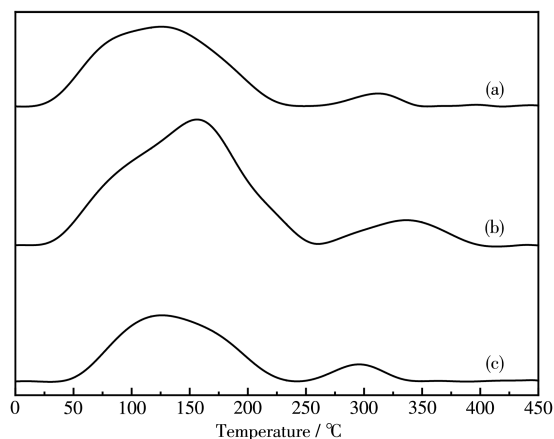


Fig.4 Plots of NH_3 -TPD signal against temperature for HT-as (a), HT-dh (b), and HT-rh (c)

2.4 Morphological analyses of Ni-Fe HTLCs

The dehydration and rehydration hardly lead to a significant change in the morphology of Ni-Fe HTLCs, and thus HT-as was used as typical sample to analyze the morphological characteristics of the catalysts. As shown in Fig. 5, the angular sheets of Ni-Fe HTLCs were clearly observed. The lamellar morphology of irregularly shaped particles was formed by the stacked thin flakes, indicating that successful preparation of Ni-Fe HTLCs with structural characteristics of hydrotalcites.

2.5 Catalytic performance

As shown in Fig.6, the FGA conversion increased

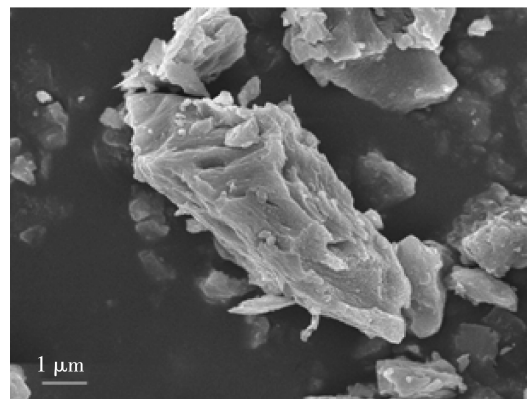


Fig.5 SEM image of HT-as

significantly with the increasing reaction time and then reached to a maximum after about 5 h. The maximum conversions were observed in the following order: HT-dh (95.1%) > HT-as (81.4%) > HT-rh (77.8%), indicating high activity of HT-dh for furfural acetalization. The result is consistent with the change in the amount of acid sites in the three samples. The acidity of weak acid sites in HT-dh was much higher compared with HT-as and HT-rh, and moreover the structure of weak acid sites in HT-dh was changed by dehydration. Therefore, weak acid sites of the dehydrated Ni-Fe HTLCs play a major role in furfural acetalization. The selectivity of HT-dh, HT-as, or HT-rh to FGA was always higher than 97%, indicating that the side-reactions of furfural is difficult to undergo during acetalization reaction at room temperature. In comparison with HT-as, the lower activity of HT-rh results from its smaller specific surface area that is caused by incomplete recovery of hydrotalcite structure. NO_3^- ions intercalating between the layers of Ni-Fe HTLCs can restrain the diffusion of organic molecules into interlayer space by steric hindrance but promote water occupying the remaining space of the interlayer by hydration. However, it is inevitable that a small quantity of organic molecules diffuses into the interlayer space during furfural acetalization, which may hinder the structural recovery of Ni-Fe HTLCs during rehydration. Analyses of water content in the products showed that 91.2% of the resulting water was absorbed by HT-dh, and the residual water may be captured by excessive ethylene glycol through hydrogen bonding. The amount of water absorbed by HT-as or HT-rh was negligible. Hence,

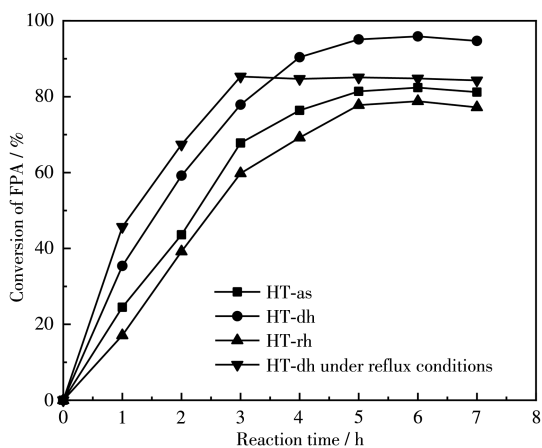


Fig.6 Conversion of FGA for all samples

the resulting water was mainly absorbed by interlayer of HT-rh, and HT-rh showed strong selective absorption of H₂O during furfural acetalization. In summary, the high activity of HT-dh for furfural acetalization results from high acidity of weak acid sites and strong dewaterability.

Under reflux conditions, the furfural acetalization over HT-dh was carried out as a contrast. As shown in Fig. 6, the FGA conversion increased to a maximum after about 3 h, and the maximum conversion reached to 85.3%. However, the selectivity of HT-dh to FGA was merely 41.4% under reflux conditions, and the color of the mixture changed from transparent to isabelle. The homopolymerization and oxidation of furfural at high temperatures may lead to the complex mixture of by-products. The abundant by-products hindered heat and mass transfer, and it is inevitable that the catalysts and reactants were encapsulated by the polymers. Accordingly, the resulting by-products under reflux conditions have negative effects on conversion of furfural and selectivity of the catalyst.

3 Conclusions

In summary, the dehydrated Ni-Fe HTLCs containing NO₃⁻ ions were synthesized by the coprecipitation method and investigated by XRD, FTIR, NH₃-TPD, and nitrogen adsorption-desorption measurements. The dehydrated Ni-Fe HTLCs showed good catalytic activity and strong dewaterability for furfural acetalization reaction. The weak acid sites play an important in the catalytic activity of Ni-Fe HTLCs. Dehydra-

tion leads to an increase in acidity of the acid sites possibly due to the decrease in electronic cloud density of the metal cations in layers of Ni-Fe HTLCs. The removal of interlayer water leads to the increase in electronic repulsion among NO₃⁻ ions, which alters the structure of metal complex in a layer of Ni-Fe HTLCs. The structure of dehydrated Ni-Fe HTLCs cannot completely recover after rehydration during furfural acetalization, because the organic molecules diffusing into interlayer space of Ni-Fe HTLCs may hinder the structural recovery.

Acknowledgements: This work is financially supported by National Natural Science Foundation of China (Grant No.22108161), Shanxi Province Science Foundation for Youths (Grant No. 201901D211297) and Shanxi Dadi Environment Investment Holdings Co. Ltd. (Grant No.228023901039).

References:

- [1] Climent M J, Corma A, Iborra S. Conversion of Biomass Platform Molecules into Fuel Additives and Liquid Hydrocarbon Fuels. *Green Chem.*, **2014**,**16**(2):516-547
- [2] Mullen C A, Boateng A A. Chemical Composition of Bio-Oils Produced by Fast Pyrolysis of two Energy Crops. *Energy Fuels*, **2008**,**22**:2104-2109
- [3] Zhang L, Liu R H, Yin R Z, Mei Y F. Upgrading of Bio-oil from Biomass Fast Pyrolysis in China: A Review. *Renewable Sustainable Energy Rev.*, **2013**,**24**:66-72
- [4] Tarazanov S V, Grigor'eva E V, Titarenko M A, Klimov N A, Ershov M A, Nikul'shin P A. Furfural Dipropyl Acetal as a New Fuel Additive: Synthesis and Properties. *Russ. J. Appl. Chem.*, **2018**,**91**(12):1968-1973
- [5] Piasecki A. Acetals and Ethers-XIII Reaction Products of 2-Butenal with Ethylene Glycol. *Tetrahedron*, **1984**,**40**(23):4893-4896
- [6] Reddy N R, Kumar R, Baskaran S. A Direct Method for the Efficient Synthesis of Benzylidene Acetal at Room Temperature. *Eur. J. Org. Chem.*, **2019**(7):1548-1552
- [7] da Silva M J, Teixeira M G, Natalino R. Highly Selective Synthesis under Benign Reaction Conditions of Furfural Dialkyl Acetal using SnCl₂ as a Recyclable Catalyst. *New J. Chem.*, **2019**,**43**:8606-8612
- [8] Climent M J, Corma A, Velly A. Synthesis of Hyacinth, Vanilla, and Blossom Orange Fragrances: the Benefit of Using Zeolites and Delaminated Zeolites as Catalysts. *Appl. Catal. A*, **2004**,**263**(2):155-161
- [9] Silveira C C, Mendes S R, Ziembowicz F I, Lenardão E J, Perin G. The Use of Anhydrous CeCl₃ as a Recyclable and Selective Catalyst

- for the Acetalization of Aldehydes and Ketones. *J. Braz. Chem. Soc.*, **2010**, **21**(2):371-374
- [10] Kanai S, Nagahara I, Kita Y, Kamata K, Hara M. A Bifunctional Cerium Phosphate Catalyst for Chemoselective Acetalization. *Chem. Sci.*, **2017**, **8**(4):3146-3153
- [11] Augustine J K, Bombrun A, Sauer W H B, Vijaykumar P. Highly Efficient and Chemoselective Acetalization and Thioacetalization of Aldehydes Catalyzed by Propylphosphonic Anhydride (@T3P) at Room Temperature. *Tetrahedron Lett.*, **2012**, **53**(37):5030-5033
- [12] Lipshutz B H, Pollart D, Monforte J, Kotsuki H. Pd(III)-Catalyzed Acetal Ketal Hydrolysis Exchange - Reactions. *Tetrahedron Lett.*, **1985**, **26**(6):705-708
- [13] Beydoun K, Klankermayer J. Ruthenium - Catalyzed Synthesis of Cyclic and Linear Acetals by the Combined Utilization of CO₂, H₂, and Biomass Derived Diols. *Chem. Eur. J.*, **2019**, **25**:11412-11415
- [14] Li Y H, Zhang X J, Ren T R, Zhou J J. New Catalytic Methods for the Preparation of Acetals from Alcohols and Aldehydes. *Synth. Commun.*, **2006**, **36**:1679-1685
- [15] Valente J S, Rodriguez-Gattorno G, Valle-Orta M, Torres-Garcia E. Thermal Decomposition Kinetics of MgAl Layered Double Hydroxides. *Mater. Chem. Phys.*, **2012**, **133**:621-629
- [16] Duan X, Evans D G. *Layered Double Hydroxides: Structure and Bonding*. Berlin: Springer, **2006**:124-126
- [17] Rives V. *Layered Double Hydroxides: Present and Future*. New York: Nova Science Publishers, **2001**:213-217
- [18] Cavani F, Trifirb F, Vaccari A. Hydrotalcite-Type Anionic Clays: Preparation, Properties and Applications. *Catal. Today*, **1991**, **11**:173-301
- [19] Vaccari A. Clays and Catalysis: A Promising Future. *Appl. Clay Sci.*, **1999**, **14**(4):161-198
- [20] Rives V, Kannan S. Layered Double Hydroxides with the Hydrotalcite-Type Structure Containing Cu²⁺, Ni²⁺ and Al³⁺. *J. Mater. Chem.*, **2000**, **10**:489-495
- [21] Allmann R. The Crystal Structure of Pyroaurite. *Acta Crystallogr.*, **1968**, **B24**:972-977
- [22] Jing F L, Zhang Y Y, Luo S Z, Chu W, Qian W Z. Nano-Size MZnAl (M=Cu, Co, Ni) Metal Oxides Obtained by Combining Hydrothermal Synthesis with Urea Homogeneous Precipitation Procedures. *Appl. Clay Sci.*, **2010**, **48**(1/2):203-207
- [23] Tanaka T, Kameshima Y, Nishimoto S, Miyake M. Determination of Carbonate Ion Contents in Layered Double Hydroxides by FTIR Spectrometry. *Anal. Methods*, **2012**, **4**(12):3925-3927
- [24] Chimentão R J, Abelló S, Medina F, Llorca J, Sueiras J E, Cesteros Y, Salagre P. Defect-Induced Strategies for the Creation of Highly Active Hydrotalcites in Base-Catalyzed Reactions. *J. Catal.*, **2007**, **252**(2):249-257
- [25] Carlino S, Hudson M J. Reaction of Molten Sebacic Acid with a Layered (Mg/Al) Double Hydroxide. *J. Mater. Chem.*, **1994**, **4**(1):99-104
- [26] Rives V. Characterisation of Layered Double Hydroxides and Their Decomposition Products. *Mater. Chem. Phys.*, **2002**, **75**(1/2/3): 19-25